

Exploring Rapidity-Even Dipolar Flow in Isobaric Collisions at RHIC

Niseem Magdy^{1,2,*} and Roy Lacey^{2,3}

¹*Center for Frontiers in Nuclear Science at the State University of New York, Stony Brook, NY 11794, USA*

²*Department of Chemistry, the State University of New York, Stony Brook, New York 11794, USA*

³*Department of Physics, Stony Brook University, Stony Brook, NY 11794*

Employing the AMPT transport model, we investigate the response of the rapidity-even dipolar flow (v_1^{even}) and its associated Global Momentum Conservation (GMC) parameter K to structural disparities within ^{96}Ru and ^{96}Zr nuclei. We analyze $\text{Ru} + \text{Ru}$ and $\text{Zr} + \text{Zr}$ collisions at a center-of-mass energy of $\sqrt{s_{NN}} = 200$ GeV. Our analysis demonstrates that the eccentricity ε_1 , v_1^{even} and K exhibit subtle yet discernible sensitivity to the input nuclear structure distinctions between ^{96}Ru and ^{96}Zr isobars. This observation suggests that measuring v_1^{even} and the GMC parameter in these isobaric collisions could serve as a means to fine-tune the comprehension of their nuclear structure disparities and offer insights to enhance the initial condition assumptions of theoretical models.

Keywords: Collectivity, correlation, shear viscosity, transverse momentum correlations

High-energy nuclear collisions at the Relativistic Heavy Ion Collider (RHIC) and the Large Hadron Collider (LHC) can produce a strongly coupled plasma of quarks and gluons (QGP). Full characterization of this hot and dense matter is central to present-day high-energy physics research. Such characterization requires detailed knowledge of the initial state in Heavy Ion Collisions (HIC) [1–16]. Numerous investigations have underscored the significance of anisotropic flow measurements, mainly focusing on n th-order flow harmonics (v_n , $n \geq 2$), as a strategic avenue for studying both the initial conditions and transport properties of the QGP such as the specific viscosity η/s or the ratio of viscosity to entropy density [17–25].

Indeed, a wealth of research endeavors has yielded a treasure trove of insights into the initial conditions shaping HIC events and the properties of the QGP produced in them. These insights have been garnered through comprehensive studies of dipolar (v_1), elliptic (v_2) and triangular (v_3) flow harmonics, encompassing not only their magnitudes, statistical variances and fluctuations but also the intricate interplay between them [10, 16, 24, 26–49].

Recent investigations have delved into the intriguing realm of exploiting collisions to constrain the structure of the colliding nuclei, specifically focusing on the ratios $\frac{v_2^{\text{Ru+Ru}}}{v_2^{\text{Zr+Zr}}}$ and $\frac{v_3^{\text{Ru+Ru}}}{v_3^{\text{Zr+Zr}}}$ obtained from collisions involving $^{96}\text{Ru} + ^{96}\text{Ru}$ and $^{96}\text{Zr} + ^{96}\text{Zr}$ [50–66]. This avenue has been explored as a means to impose constraints on the disparities in the initial-state deformation and the neutron skin of these two isobars. The motivation behind these investigations arises from the notion that, in these isobaric collisions, there is an expectation that the viscosity-related attenuation dependent on final-state multiplicity should exhibit similarities [67]. However, subtle variations in their inherent shapes and neutron distributions can lead to distinct differences in the initial-state eccen-

tricitities [68, 69], thereby giving rise to noticeable disparities in the magnitudes of v_2 and v_3 for the respective isobaric pairs.

The component of directed flow that is even in rapidity (v_1^{even}), also known as dipolar flow, arises from the interplay of initial-state fluctuations and a hydrodynamic-like expansion process [70–74]. As a result, its magnitude is influenced by both the initial-state eccentricity (ε_1) and viscous effects that are dependent on multiplicity (N_{ch}) and η/s . However, different studies suggest that v_1^{even} is less sensitive to viscous effects compared to higher-order harmonics ($n \geq 2$) [74, 75]. Given these considerations, it is valuable to explore whether the subtle variations in intrinsic deformations and neutron skin thickness among the isobars will lead to characteristic distinctions in the behavior of v_1^{even} between them. Thus, we pose the question: *To what extent will the difference in the initial state between $\text{Ru} + \text{Ru}$ and $\text{Zr} + \text{Zr}$ will impact the v_1^{even} observable?*

In this investigation, we employ the multiphase transport model AMPT to analyze the behavior of both ε_1 and v_1^{even} with respect to collision centrality in scenarios involving $^{96}\text{Ru} + ^{96}\text{Ru}$ and $^{96}\text{Zr} + ^{96}\text{Zr}$ collisions at $\sqrt{s_{NN}} = 200$ GeV. These analyses take into account the distinct intrinsic deformations and neutron skin disparities assumed to be inherent to these isobaric species.

The AMPT model [76] is a comprehensive simulation framework widely utilized to delve into the complexities of relativistic heavy-ion collisions [76–83]. In this particular study, we generate AMPT events that incorporate the string-melting option. Within the AMPT framework, the Glauber model is employed to define the shape and radial distribution of the colliding nuclei, employing a deformed Woods-Saxon distribution [84]:

$$\rho(r, \theta, \phi) \propto \frac{1}{1 + e^{(r-R(\theta, \phi))/a_0}}, \quad (1)$$

$$R(\theta, \phi) = R_0(1 + \beta_2 Y_2^0(\theta, \phi) + \beta_3 Y_3^0(\theta, \phi)). \quad (2)$$

Here, the nuclear surface $R(\theta, \phi)$ incorporates quadrupole and octupole deformations regulated by β_2 and β_3 , respectively, and the parameters R_0 and a_0 represent the

* niseemm@gmail.com

half-height radius and nuclear skin thickness. In collisions, the projectile and target nuclei are rotated event-by-event randomly along the polar and azimuthal directions. The Woods-Saxon parameter sets for ^{96}Ru and ^{96}Zr employed in our analysis are summarized in Table I [85].

AMPT-set	R_0	a_0	β_2	β_3
$^{96}\text{Ru}+^{96}\text{Ru}$ (Case-1)	5.09	0.46	0.162	0.00
$^{96}\text{Zr}+^{96}\text{Zr}$ (Case-2)	5.02	0.52	0.06	0.20
$^{96}\text{Zr}+^{96}\text{Ru}$ (Case-3)	5.09	0.46	0.06	0.20
$^{96}\text{Zr}+^{96}\text{Zr}$ (Case-4)	5.09	0.46	0.06	0.00

TABLE I. Summary of the Woods-Saxon parameters for ^{96}Ru and ^{96}Zr employed in the AMPT studies.

The dipole asymmetry or eccentricity ε_1 of the collision systems, was obtained as a function of centrality for the respective cases outlined in Table I, as [70–72]:

$$\varepsilon_1 \equiv -\frac{\langle r^3 \cos(\phi - \psi_{1,3}) \rangle}{\langle r^3 \rangle} \quad (3)$$

$$\psi_{1,3} \equiv \text{atan2}(\langle r^3 \sin \phi \rangle, \langle r^3 \cos \phi \rangle) + \pi \quad (4)$$

where the averaging is performed over the initial energy density.

Within the same AMPT framework, the HIJING model is employed to generate hadrons, which are then transformed into their constituent quarks and anti-quarks. The subsequent space-time evolution of these particles is determined using the ZPC Parton cascade model [86], which incorporates the parton-scattering cross-section:

$$\sigma_{pp} = \frac{9\pi\alpha_s^2}{2\mu^2}, \quad (5)$$

where α_s denotes the QCD coupling constant and μ is the screening mass in the partonic matter; these parameters collectively shape the expansion dynamics of the collision systems [86]. Collisions were simulated for a fixed value of $\sigma_{pp} = 2.8$ (mb) [87, 88]. Thus, the AMPT model amalgamates several contributing factors: (i) the initial-state eccentricity, (ii) the initial Parton-production stage governed by the HIJING model [89, 90], (iii) a Parton-scattering stage, (iv) the process of hadronization through coalescence, and finally, (v) a phase that encompasses interactions among the generated hadrons [91].

The coefficients v_1^{even} were determined by studying the transverse momentum (p_T) and collision centrality dependencies using a two-particle correlation technique [75, 92]. The analysis focused on charged hadrons within a transverse momentum range of $0.2 < p_T < 3.0$ GeV/c and a pseudorapidity acceptance of $|\eta| < 1.0$. Additionally, simulated events were categorized into various

collision centrality classes based on the collision's multiplicity.

Initially, the correlation function method [93] was employed to construct the two-particle $\Delta\phi$ correlations,

$$C_r(\Delta\phi, \Delta\eta) = \frac{(dN/d\Delta\phi)_{\text{same}}}{(dN/d\Delta\phi)_{\text{mixed}}}, \quad (6)$$

where $\Delta\eta = \eta_a - \eta_b$ represents the pseudorapidity difference between particles a and b . The terms $(dN/d\Delta\phi)_{\text{same}}$ and $(dN/d\Delta\phi)_{\text{mixed}}$ denote the normalized azimuthal distribution for particle pairs originating from the same and mixed events, respectively. To mitigate short-range non-flow correlations [70, 75, 92–94], a condition of $|\Delta\eta| > 0.7$ was applied to the pairs, which helps reduce contributions from resonance decays, Bose-Einstein correlations, and jets. However, it's important to note that long-range non-flow correlations [75, 92] (such as those arising from jets and global momentum conservation (GMC)) still persist.

Subsequently, the values of v_{11} were deduced from the correlation functions (Eq.6) as:

$$v_{11} = \frac{\sum_{\Delta\phi} C_r(\Delta\phi) \cos(n\Delta\phi)}{\sum_{\Delta\phi} C_r(\Delta\phi)}, \quad (7)$$

and simultaneously fitted as a function of p_T^a and p_T^b to extract the v_1^{even} :

$$v_{11}(p_T^a, p_T^b) = v_1^{\text{even}}(p_T^a) v_1^{\text{even}}(p_T^b) - K p_T^a p_T^b. \quad (8)$$

Here the parameter K takes into account the long-range non-flow from GMC [75, 92, 94, 95]. It is anticipated to be correlated with the average multiplicity $\langle N_{\text{ch}} \rangle$ and the variance of the transverse momentum across the full phase space (i.e., $K \propto 1/(\langle N_{\text{ch}} \rangle \langle p_T^2 \rangle)$).

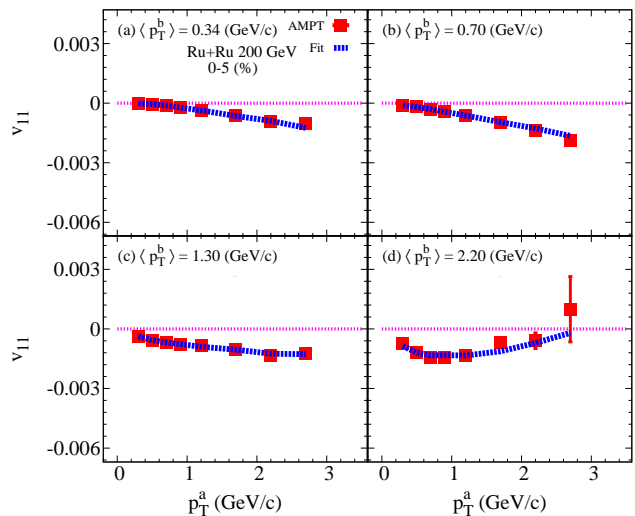


FIG. 1. v_{11} vs. p_T^a for several p_T^b for 0-5% central Ru+Ru collisions [Case-1]. The curves indicate the result of the simultaneous fit with Eq. (8).

For a single centrality selection, the v_{11} matrix is N -by- M in size, and we fit it using the right-hand side of

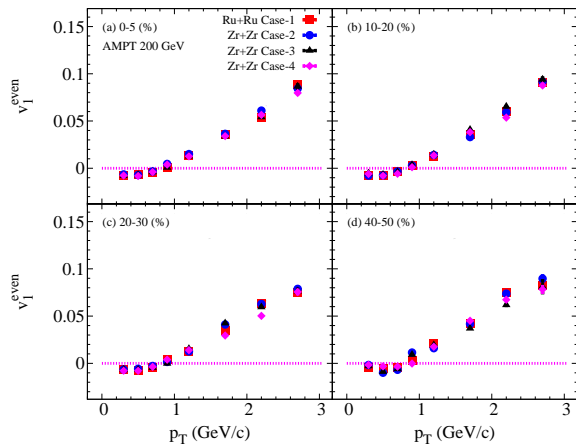


FIG. 2. The extracted v_1^{even} vs. p_T for 0-5% (a), 10-20% (b), 20-30% (c), and 40-50% (d) Ru + Ru and Zr + Zr collisions, for the respective cases in Table I as indicated.

Eq. 8. The fit function encompasses $N+1$ parameters: N parameters correspond to $v_1^{\text{even}}(p_T)$, and the parameter K accounts for momentum conservation [96]. Figure 1 illustrates the efficacy of the fitting approach for 0-5% central Ru+Ru collisions. The curves in each panel depict the fits, showcasing how the v_{11} points evolve from negative to positive values as the selection range for p_T^b is increased. This trend for v_{11} serves as an important constraint for the fits.

The extracted v_1^{even} values for the respective cases in Table I are depicted as functions of p_T and centrality in Fig. 2. They display a characteristic pattern [75]: a transition from negative $v_1^{\text{even}}(p_T)$ at low p_T to positive $v_1^{\text{even}}(p_T)$ for $p_T \gtrsim 1$ GeV/c, with a crossing point that gradually shifts with increasing centrality. This behavior results from the requirement that the net transverse momentum of the system is zero, implying that the hydrodynamic flow direction of low p_T particles opposes that of high p_T particles. Additionally, the computations reveal small distinctions among the different AMPT Cases, which will be elaborated upon in subsequent discussions.

The corresponding values of the GMC parameter K are shown in Fig 3. These values reveal a linear correlation between K and $\langle N_{\text{ch}} \rangle^{-1}$, mirroring the observed trend in experimental data [67], albeit with a more modest slope in our model results. Furthermore, the slope of K with respect to $\langle N_{\text{ch}} \rangle^{-1}$ is influenced by the nuclear structure parameters delineated in Table I. This dependence indicates a subtle yet distinguishable disparity in slopes for Case-1 through Case-4, with a maximum difference of $\sim 4\% \pm 1.4\%$ between Case-1 and Case-2. These insights imply that conducting meticulous comparisons of K vs. $\langle N_{\text{ch}} \rangle^{-1}$ for data and theoretical models could offer a nuanced understanding of the GMC effect within theoretical frameworks. Furthermore, such analyzes could serve as a valuable tool for refining our grasp of the nuclear structure disparities between the Ru and Zr isobars.

To gain a deeper insight into the potential influence

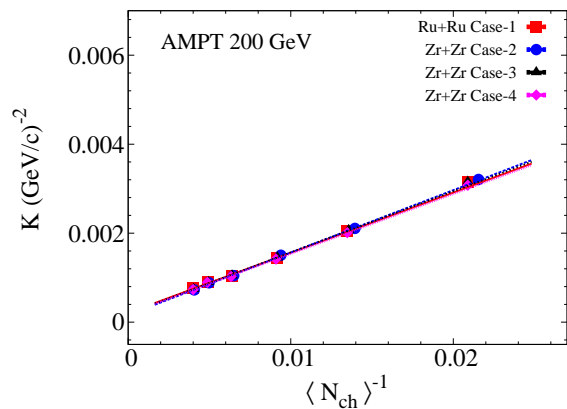


FIG. 3. K values vs. $\langle N_{\text{ch}} \rangle^{-1}$ for the respective cases in Table I. The lines show linear fits to the results.

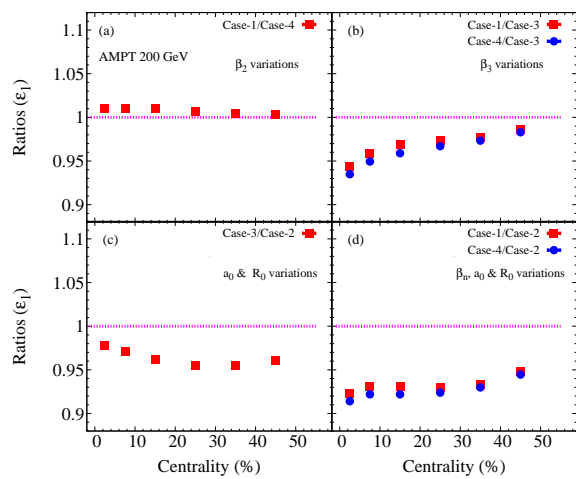


FIG. 4. The centrality dependence of the initial state ϵ_1 ratios for Case-1/Case-4 (a), Case-1/Case-3 and Case-4/Case-3 (b), Case-3/Case-2 (c), and Case-1/Case-2 and Case-4/Case-2 (d).

stemming from intrinsic deformation variations and neutron skin disparities between the isobaric nuclei, we investigated the ratios of ϵ_1 and v_1^{even} across the different scenarios outlined in Table I. The centrality dependence of the ϵ_1 ratios are shown in Fig. 4, with the intent of deciphering the interplay of distinct nuclear structure effects and capturing the sensitivity of ϵ_1 to β_n , R_0 , and a_0 .

Analyzing the panels in Fig. 4, we find that the Case-1/Case-4 ratio (panel a) reveals a resilience of ϵ_1 against variations in β_2 , as anticipated for a fluctuation-driven ϵ_1 . Contrarily, panels (b) show the Case-1/Case-3 and Case-4/Case-3 ratios, shedding light on a $\sim 3.0\%$ difference in central collisions, which gradually diminishes as the collisions become more peripheral. This trend underscores the dependency of ϵ_1 on β_3 . Complementary insights into the effects of a_0 and R_0 on ϵ_1 are gleaned from the Case-3/Case-2 ratios in panel (c), displaying an opposing trend compared to panel (b) with differences ranging from $\sim 1 - 3\%$ based on centrality.

Combining the influences of β_3 , a_0 , and R_0 on ϵ_1 , panel (d) showcases the Case-1/Case-2 and Case-4/Case-2 ratios. These ratios indicate a $\sim 4.0\%$ variation in central collisions that steadily diminishes as collisions become more peripheral. These findings collectively highlight the subtle but discernible sensitivity of the ϵ_1 ratios to nuclear structure disparities between the two isobaric nuclei. This prompts the question: "How does this sensitivity translate into the corresponding v_1^{even} ratios?"

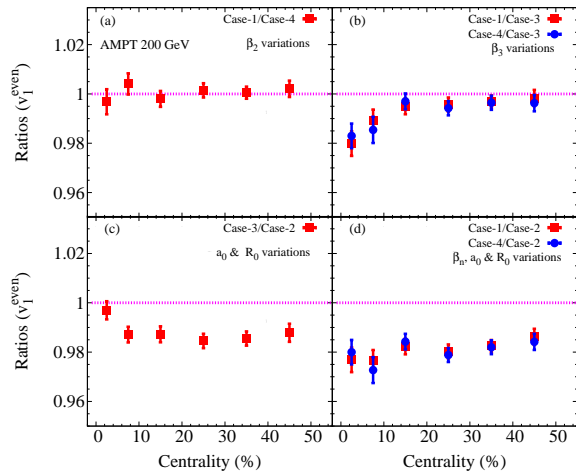


FIG. 5. Centrality dependence of the integrated ($0.2 < p_T < 0.9$ GeV/c) v_1^{even} ratios between Case-1/Case-4 (a), Case-1/Case-3 and Case-4/Case-3 (b), Case-3/Case-2 (c), and Case-1/Case-2 and Case-4/Case-2 (d).

The centrality-dependent v_1^{even} ratios for the various AMPT cases are shown in Fig. 5 for the $0.2 < p_T < 0.9$ GeV/c range. These ratios reflect patterns akin to those observed for the ϵ_1 ratios in Fig. 4, albeit with reduced magnitudes. The Case-1/Case-4 ratio suggests the insensitivity of v_1^{even} to β_2 variations. In contrast, the Case-1/Case-3 and Case-4/Case-3 ratios hint at a $\sim 2\%$ distinction in central collisions, which quickly diminishes towards peripheral collisions, showcasing the susceptibility of v_1^{even} to β_3 variations. Panels (c) and (d) illuminate the subtle but perceptible response of v_1^{even} to variations in a_0 and R_0 and their combined impact. These distinctive trends suggests that v_1^{even} measurements for Ru + Ru and Zr + Zr can serve as crucial constraints in delineating the nuclear structure differences between these isobaric nuclei.

The magnitude of the slope in $\ln(v_1^{\text{even}}/\epsilon_1)$ vs. $\langle N_{\text{ch}} \rangle^{-1/3}$ provides valuable insights into the viscous coefficient of the generated medium [67, 97]. As the effective viscous coefficient remains consistent across the scenarios outlined in Table I, one can reasonably expect similar slope magnitudes in these simulated outcomes. As shown in Fig. 6, our results indeed exhibit this consistency, implying that comparing $\ln(v_1^{\text{even}}/\epsilon_1)$ vs. $\langle N_{\text{ch}} \rangle^{-1/3}$ between Ru + Ru and Zr + Zr for experimental data and ϵ_1 for the different cases could serve as an additional avenue to further refine the distinction of nuclear structure between these isobaric nuclei.

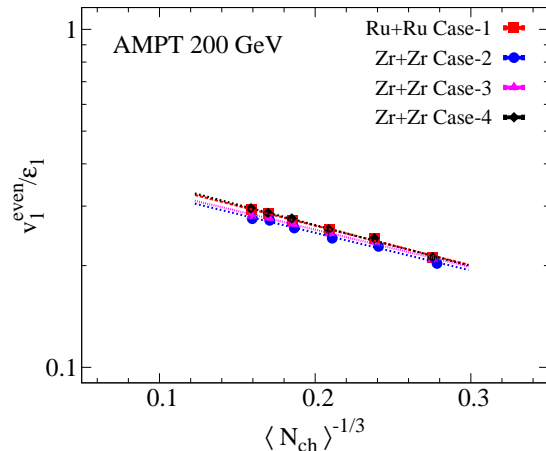


FIG. 6. Comparison of $v_1^{\text{even}}/\epsilon_1$ vs. $\langle N_{\text{ch}} \rangle^{-1/3}$ for the respective cases in Table I as indicated. The lines show the fits to the results.

Our investigation revealed a maximum deviation of 2% and 4% between Ru + Ru and Zr + Zr for v_1^{even} and the parameter K , respectively. This observation prompts the question of whether such differences can be feasibly detected experimentally. In 2018, the STAR experiment at RHIC collected 1.2 billion minimum-bias events for each collision system (Ru + Ru and Zr + Zr). These comprehensive data sets were gathered to (i) minimize statistical uncertainties in individual system measurements and (ii) mitigate systematic uncertainties in the Ru + Ru and Zr + Zr ratios [50]. Moreover, analysis conducted by the STAR experiment indicated that differences between the two systems could be discerned at levels approaching fractions of a percent in anisotropic flow measurements. Consequently, we advocate for the implementation of our proposed study by the STAR experiment at RHIC.

In summary, we have employed the two-particle correlation functions method within the AMPT model framework to examine the responsiveness of the rapidity-even dipolar flow (v_1^{even}) and its associated Global Momentum Conservation parameter K to inherent structural distinctions within ^{96}Ru and ^{96}Zr nuclei. Our model-based investigations have revealed modest yet discernible sensitivity to nuclear structure variations between the two isobars. This underscores the potential significance of measuring v_1^{even} and the GMC parameter in isobaric collisions at RHIC, offering a practical means to refine the theoretical model inputs essential for comprehending the nuclear structure disparities between the ^{96}Ru and ^{96}Zr isobars.

ACKNOWLEDGMENTS

The authors thank Dr. Emily Racow for the valuable discussions. This research is supported by the US Department of Energy, Office of Nuclear Physics (DOE NP),

-
- [1] P. Danielewicz, R. A. Lacey, P. Gossiaux, C. Pinkenburg, P. Chung, J. Alexander, and R. McGrath, *Phys. Rev. Lett.* **81**, 2438 (1998), arXiv:nucl-th/9803047.
- [2] K. Ackermann *et al.* (STAR), *Phys. Rev. Lett.* **86**, 402 (2001), arXiv:nucl-ex/0009011.
- [3] K. Adcox *et al.* (PHENIX), *Phys. Rev. Lett.* **89**, 212301 (2002), arXiv:nucl-ex/0204005 [nucl-ex].
- [4] U. W. Heinz and P. F. Kolb, *Statistical QCD. Proceedings, International Symposium, Bielefeld, Germany, August 26-30, 2001*, *Nucl. Phys.* **A702**, 269 (2002), arXiv:hep-ph/0111075 [hep-ph].
- [5] T. Hirano, U. W. Heinz, D. Kharzeev, R. Lacey, and Y. Nara, *Phys. Lett.* **B636**, 299 (2006), arXiv:nucl-th/0511046 [nucl-th].
- [6] P. Huovinen, P. F. Kolb, U. W. Heinz, P. V. Ruuskanen, and S. A. Voloshin, *Phys. Lett.* **B503**, 58 (2001).
- [7] T. Hirano and K. Tsuda, *Phys. Rev.* **C66**, 054905 (2002), arXiv:nucl-th/0205043.
- [8] P. Romatschke and U. Romatschke, *Phys. Rev. Lett.* **99**, 172301 (2007), arXiv:0706.1522 [nucl-th].
- [9] M. Luzum, *J. Phys.* **G38**, 124026 (2011), arXiv:1107.0592 [nucl-th].
- [10] H. Song, S. A. Bass, U. Heinz, T. Hirano, and C. Shen, *Phys. Rev. Lett.* **106**, 192301 (2011), [Erratum: *Phys. Rev. Lett.* **109**, 139904 (2012)], arXiv:1011.2783 [nucl-th].
- [11] J. Qian, U. W. Heinz, and J. Liu, *Phys. Rev.* **C93**, 064901 (2016), arXiv:1602.02813 [nucl-th].
- [12] B. Schenke, S. Jeon, and C. Gale, *Phys. Lett.* **B702**, 59 (2011), arXiv:1102.0575 [hep-ph].
- [13] D. Teaney and L. Yan, *Phys. Rev.* **C86**, 044908 (2012), arXiv:1206.1905 [nucl-th].
- [14] F. G. Gardim, F. Grassi, M. Luzum, and J.-Y. Ollitrault, *Phys. Rev. Lett.* **109**, 202302 (2012), arXiv:1203.2882 [nucl-th].
- [15] R. A. Lacey, D. Reynolds, A. Taranenko, N. N. Ajitanand, J. M. Alexander, F.-H. Liu, Y. Gu, and A. Mwai, *J. Phys.* **G43**, 10LT01 (2016), arXiv:1311.1728 [nucl-ex].
- [16] N. Magdy, *Phys. Rev. C* **107**, 024905 (2023), arXiv:2210.14091 [nucl-th].
- [17] D. Teaney, *Phys. Rev.* **C68**, 034913 (2003), arXiv:nucl-th/0301099 [nucl-th].
- [18] R. A. Lacey and A. Taranenko, *Correlations and fluctuations in relativistic nuclear collisions. Proceedings, 2nd International Workshop, CFRNC2006, Florence, Italy, July 7-9, 2006*, *PoS CFRNC2006*, 021 (2006), arXiv:nucl-ex/0610029 [nucl-ex].
- [19] H. Song, S. A. Bass, and U. Heinz, *Phys. Rev.* **C83**, 054912 (2011), arXiv:1103.2380 [nucl-th].
- [20] B. Alver and G. Roland, *Phys. Rev.* **C81**, 054905 (2010), [Erratum: *Phys. Rev.* **C82**, 039903 (2010)], arXiv:1003.0194 [nucl-th].
- [21] B. Schenke, S. Jeon, and C. Gale, *Phys. Rev. Lett.* **106**, 042301 (2011), arXiv:1009.3244 [hep-ph].
- [22] C. Shen, U. Heinz, P. Huovinen, and H. Song, *Phys. Rev.* **C82**, 054904 (2010), arXiv:1010.1856 [nucl-th].
- [23] H. Niemi, G. Denicol, P. Huovinen, E. Molnar, and D. Rischke, *Phys. Rev.* **C86**, 014909 (2012), arXiv:1203.2452 [nucl-th].
- [24] G.-Y. Qin, H. Petersen, S. A. Bass, and B. Muller, *Phys. Rev.* **C82**, 064903 (2010), arXiv:1009.1847 [nucl-th].
- [25] N. Magdy, *Universe* **9**, 107 (2023), arXiv:2302.10373 [nucl-th].
- [26] J. Adam *et al.* (STAR), *Phys. Lett.* **B783**, 459 (2018), arXiv:1803.03876 [nucl-ex].
- [27] J. Adam *et al.* (ALICE), *Phys. Rev. Lett.* **117**, 182301 (2016), arXiv:1604.07663 [nucl-ex].
- [28] L. Adamczyk *et al.* (STAR), *Phys. Rev.* **C98**, 034918 (2018), arXiv:1701.06496 [nucl-ex].
- [29] Z. Qiu and U. W. Heinz, *Phys. Rev.* **C84**, 024911 (2011), arXiv:1104.0650 [nucl-th].
- [30] A. Adare *et al.* (PHENIX), *Phys. Rev. Lett.* **107**, 252301 (2011), arXiv:1105.3928 [nucl-ex].
- [31] G. Aad *et al.* (ATLAS), *Phys. Rev.* **C90**, 024905 (2014), arXiv:1403.0489 [hep-ex].
- [32] G. Aad *et al.* (ATLAS), *Phys. Rev.* **C92**, 034903 (2015), arXiv:1504.01289 [hep-ex].
- [33] N. Magdy (STAR), *Proceedings, 27th International Conference on Ultrarelativistic Nucleus-Nucleus Collisions (Quark Matter 2018): Venice, Italy, May 14-19, 2018*, *Nucl. Phys.* **A982**, 255 (2019), arXiv:1807.07638 [nucl-ex].
- [34] B. Alver *et al.* (PHOBOS), *Phys. Rev.* **C77**, 014906 (2008), arXiv:0711.3724 [nucl-ex].
- [35] B. Alver *et al.* (PHOBOS), *Phys. Rev.* **C81**, 034915 (2010), arXiv:1002.0534 [nucl-ex].
- [36] J.-Y. Ollitrault, A. M. Poskanzer, and S. A. Voloshin, *Phys. Rev.* **C80**, 014904 (2009), arXiv:0904.2315 [nucl-ex].
- [37] N. Magdy, *Phys. Rev. C* **106**, 044911 (2022), arXiv:2207.04530 [nucl-th].
- [38] M. Abdallah *et al.* (STAR), *Phys. Rev. Lett.* **129**, 252301 (2022), arXiv:2201.10365 [nucl-ex].
- [39] L. Adamczyk *et al.* (STAR), *Phys. Rev. C* **94**, 034908 (2016), arXiv:1601.07052 [nucl-ex].
- [40] L. Adamczyk *et al.* (STAR), *Phys. Rev. C* **93**, 014907 (2016), arXiv:1509.08397 [nucl-ex].
- [41] L. Adamczyk *et al.* (STAR), *Phys. Rev. Lett.* **115**, 222301 (2015).

- [42] L. Adamczyk *et al.* (STAR), Phys. Rev. Lett. **116**, 112302 (2016), arXiv:1601.01999 [nucl-ex].
- [43] J. Adam *et al.* (STAR), Phys. Rev. Lett. **122**, 172301 (2019), arXiv:1901.08155 [nucl-ex].
- [44] H. Niemi, G. S. Denicol, H. Holopainen, and P. Huovinen, Phys. Rev. **C87**, 054901 (2013), arXiv:1212.1008 [nucl-th].
- [45] F. G. Gardim, J. Noronha-Hostler, M. Luzum, and F. Grassi, Phys. Rev. **C91**, 034902 (2015), arXiv:1411.2574 [nucl-th].
- [46] J. Fu, Phys. Rev. **C92**, 024904 (2015).
- [47] H. Holopainen, H. Niemi, and K. J. Eskola, Phys. Rev. **C83**, 034901 (2011), arXiv:1007.0368 [hep-ph].
- [48] C. Gale, S. Jeon, B. Schenke, P. Tribedy, and R. Venugopalan, Phys. Rev. Lett. **110**, 012302 (2013), arXiv:1209.6330 [nucl-th].
- [49] P. Liu and R. A. Lacey, Phys. Rev. **C 98**, 021902 (2018), arXiv:1802.06595 [nucl-ex].
- [50] M. Abdallah *et al.* (STAR), Phys. Rev. **C 105**, 014901 (2022), arXiv:2109.00131 [nucl-ex].
- [51] H. Li, H.-j. Xu, J. Zhao, Z.-W. Lin, H. Zhang, X. Wang, C. Shen, and F. Wang, Phys. Rev. **C 98**, 054907 (2018), arXiv:1808.06711 [nucl-th].
- [52] H. Li, H.-j. Xu, Y. Zhou, X. Wang, J. Zhao, L.-W. Chen, and F. Wang, Phys. Rev. Lett. **125**, 222301 (2020), arXiv:1910.06170 [nucl-th].
- [53] H.-j. Xu, H. Li, X. Wang, C. Shen, and F. Wang, Phys. Lett. **B 819**, 136453 (2021), arXiv:2103.05595 [nucl-th].
- [54] H.-j. Xu, H. Li, Y. Zhou, X. Wang, J. Zhao, L.-W. Chen, and F. Wang, Phys. Rev. **C 105**, L011901 (2022), arXiv:2105.04052 [nucl-th].
- [55] H.-j. Xu, W. Zhao, H. Li, Y. Zhou, L.-W. Chen, and F. Wang, Phys. Rev. **C 108**, L011902 (2023), arXiv:2111.14812 [nucl-th].
- [56] S. Zhao, H.-j. Xu, Y.-X. Liu, and H. Song, Phys. Lett. **B 839**, 137838 (2023), arXiv:2204.02387 [nucl-th].
- [57] H. Xu (STAR), Acta Phys. Polon. Supp. **16**, 30 (2023), arXiv:2208.06149 [nucl-ex].
- [58] J.-f. Wang, H.-j. Xu, and F. Wang, (2023), arXiv:2305.17114 [nucl-th].
- [59] A. Dimri, S. Bhatta, and J. Jia, Eur. Phys. J. **A 59**, 45 (2023), arXiv:2301.03556 [nucl-th].
- [60] L.-M. Liu, C.-J. Zhang, J. Xu, J. Jia, and G.-X. Peng, Phys. Rev. **C 106**, 034913 (2022), arXiv:2209.03106 [nucl-th].
- [61] M. Nie, C. Zhang, Z. Chen, L. Yi, and J. Jia, (2022), arXiv:2208.05416 [nucl-th].
- [62] J. Jia, G. Giacalone, and C. Zhang, Phys. Rev. Lett. **131**, 022301 (2023), arXiv:2206.10449 [nucl-th].
- [63] J. Jia, G. Giacalone, and C. Zhang, Chin. Phys. Lett. **40**, 042501 (2023), arXiv:2206.07184 [nucl-th].
- [64] C. Zhang, S. Bhatta, and J. Jia, Phys. Rev. **C 106**, L031901 (2022), arXiv:2206.01943 [nucl-th].
- [65] J. Jia, G. Wang, and C. Zhang, Phys. Lett. **B 833**, 137312 (2022), arXiv:2203.12654 [nucl-th].
- [66] L.-M. Liu, C.-J. Zhang, J. Zhou, J. Xu, J. Jia, and G.-X. Peng, Phys. Lett. **B 834**, 137441 (2022), arXiv:2203.09924 [nucl-th].
- [67] J. Adam *et al.* (STAR), Phys. Rev. Lett. **122**, 172301 (2019), arXiv:1901.08155 [nucl-ex].
- [68] J. Jia, Phys. Rev. **C 105**, 014905 (2022), arXiv:2106.08768 [nucl-th].
- [69] G. Giacalone, J. Jia, and C. Zhang, Phys. Rev. Lett. **127**, 242301 (2021), arXiv:2105.01638 [nucl-th].
- [70] M. Luzum and J.-Y. Ollitrault, Phys. Rev. Lett. **106**, 102301 (2011), arXiv:1011.6361 [nucl-ex].
- [71] D. Teaney and L. Yan, Phys. Rev. **C83**, 064904 (2011), arXiv:1010.1876 [nucl-th].
- [72] F. G. Gardim, F. Grassi, Y. Hama, M. Luzum, and J.-Y. Ollitrault, Phys. Rev. **C83**, 064901 (2011), arXiv:1103.4605 [nucl-th].
- [73] N. Magdy (STAR), EPJ Web Conf. **171**, 16002 (2018), arXiv:1802.03869 [nucl-ex].
- [74] J. Adam *et al.* (STAR), Phys. Lett. **B 784**, 26 (2018), arXiv:1804.08647 [nucl-ex].
- [75] E. Retinskaya, M. Luzum, and J.-Y. Ollitrault, Phys. Rev. Lett. **108**, 252302 (2012), arXiv:1203.0931 [nucl-th].
- [76] Z.-W. Lin, C. M. Ko, B.-A. Li, B. Zhang, and S. Pal, Phys. Rev. **C72**, 064901 (2005), arXiv:nucl-th/0411110 [nucl-th].
- [77] G.-L. Ma and Z.-W. Lin, Phys. Rev. **C93**, 054911 (2016), arXiv:1601.08160 [nucl-th].
- [78] M. R. Haque, M. Nasim, and B. Mohanty, J. Phys. **G 46**, 085104 (2019).
- [79] P. P. Bhaduri and S. Chattopadhyay, Phys. Rev. **C 81**, 034906 (2010), arXiv:1002.4100 [hep-ph].
- [80] M. Nasim, L. Kumar, P. K. Netrakanti, and B. Mohanty, Phys. Rev. **C 82**, 054908 (2010), arXiv:1010.5196 [nucl-ex].
- [81] J. Xu and C. M. Ko, Phys. Rev. **C 83**, 021903 (2011), arXiv:1011.3750 [nucl-th].
- [82] N. Magdy, O. Evdokimov, and R. A. Lacey, J. Phys. **G 48**, 025101 (2020), arXiv:2002.04583 [nucl-ex].
- [83] Y. Guo, S. Shi, S. Feng, and J. Liao, Phys. Lett. **B 798**, 134929 (2019), arXiv:1905.12613 [nucl-th].
- [84] K. Hagino, N. W. Lwin, and M. Yamagami, Phys. Rev. **C 74**, 017310 (2006), arXiv:nucl-th/0604048.
- [85] P. Moller, J. R. Nix, W. D. Myers, and W. J. Swiatecki, Atom. Data Nucl. Data Tabl. **59**, 185 (1995), arXiv:nucl-th/9308022.
- [86] B. Zhang, Comput. Phys. Commun. **109**, 193 (1998), arXiv:nucl-th/9709009 [nucl-th].
- [87] J. Xu and C. M. Ko, Phys. Rev. **C 83**, 034904 (2011), arXiv:1101.2231 [nucl-th].
- [88] M. Nasim, Phys. Rev. **C 95**, 034905 (2017), arXiv:1612.01066 [nucl-ex].
- [89] X.-N. Wang and M. Gyulassy, Phys. Rev. **D44**, 3501 (1991).

- [90] M. Gyulassy and X.-N. Wang, *Comput. Phys. Commun.* **83**, 307 (1994), arXiv:nucl-th/9502021 [nucl-th].
- [91] B.-A. Li and C. M. Ko, *Phys. Rev.* **C52**, 2037 (1995), arXiv:nucl-th/9505016 [nucl-th].
- [92] G. Aad *et al.* (ATLAS), *Phys. Rev.* **C86**, 014907 (2012), arXiv:1203.3087 [hep-ex].
- [93] R. A. Lacey, *Proceedings, 18th International Conference on Ultra-Relativistic Nucleus-Nucleus Collisions (Quark Matter 2005): Budapest, Hungary, August 4-9, 2005*, *Nucl. Phys.* **A774**, 199 (2006), arXiv:nucl-ex/0510029 [nucl-ex].
- [94] N. Borghini, P. M. Dinh, and J.-Y. Ollitrault, *Phys. Rev.* **C62**, 034902 (2000), arXiv:nucl-th/0004026 [nucl-th].
- [95] N. Borghini, P. M. Dinh, J.-Y. Ollitrault, A. M. Poskanzer, and S. A. Voloshin, *Phys. Rev.* **C66**, 014901 (2002), arXiv:nucl-th/0202013 [nucl-th].
- [96] J. Jia, S. K. Radhakrishnan, and S. Mohapatra, *J. Phys.* **G40**, 105108 (2013), arXiv:1203.3410 [nucl-th].
- [97] P. Liu and R. A. Lacey, *Phys. Rev. C* **98**, 031901 (2018), arXiv:1804.04618 [nucl-ex].